Resonant photoemission involving super-Coster-Kronig transitions

L. C. Davis and L. A. Feldkamp
Research Staff, Ford Motor Company, Dearborn, Michigan 48121
(Received 9 February 1981)

We extend to photoemission the formal theory of the interaction of many discrete states with many continua and present three model calculations which illustrate the significant aspects of resonant photoemission. The first two models treat $3p$ core level to $3d$ band absorption, followed by super-Coster-Kronig decay ($3p^5 3d^{n+1} \rightarrow 3p^6 3d^{n-1} \epsilon f$), which interferes with the direct excitation of the $3d$ valence band. The first calculation is for a simple band model which applies approximately to Cr. No d-d interactions or atomic effects are included, yet interference characteristic of Fano resonances is clearly evident. Specifically, a strong dip in the valence-band photoemission occurs near threshold. The second model contains hole-hole interactions and exhibits a resonant two-bound-hole satellite in photoemission. The dependence of the photoemission intensity on photon energy shows a larger Fano q parameter for the satellite than for absorption, in agreement with an experiment on Ni. Further, the satellite shows strong enhancement at resonance, whereas the main line (valence-band emission) shows primarily an interference dip, as observed. The third model is for metals with filled $3d$ bands, such as Cu, Zn, ... The absorption is from $3p$ to the $4s$-$4p$ band. The resulting super-Coster-Kronig decay of the $3p$ hole gives rise to the $M_{2,3}M_{4,5}M_{4,5}$ Auger peak (fixed kinetic energy) as well as a resonant satellite at fixed binding energy. The latter is due to a singularity $[N(h\nu, E^B) \sim (E^B - E_0^B)^{-\lambda}]$ in the photoemission intensity caused by the strong interaction of the $4s$-$4p$ conduction electrons and the $3d^8$ configuration in the final state.

I. INTRODUCTION

Resonant photoemission involving super-Coster-Kronig (SCK) transitions was first observed by Guillot *et al.*[1] in Ni metal. For photon energy $h\nu$ near the threshold ($h\nu \simeq 66$ eV) at which the $3p$ core levels are excited, they found that the $3d$ electron emission is greatly enhanced. Barth, Kalkoffen, and Kunz[2] also studied the resonant behavior of the emission for various electron binding energies. As shown in Fig. 2 of Ref. 2, most of the enhancement occurs in the region of the 6-eV satellite, whereas the valence-band region exhibits an interference dip.

Dietz *et al.*[3] first explained the Fano resonance[4] which occurs at the $3p$ threshold in absorption[5,6] as well as in energy-loss measurements.[7-9] They argued, utilizing calculations by McGuire[10] of decay probabilities and matrix elements, that an interference occurs between the direct process $3p^6 3d^9 + h\nu \rightarrow 3p^6 3d^8 \epsilon f$ (in atomic notation) and the excitation involving SCK transitions $3p^6 3d^9 + h\nu \rightarrow 3p^5 3d^{10} \rightarrow 3p^6 3d^8 \epsilon f$. The interference gives rise to the characteristic Fano line shape and the strong SCK decay determines the width of the resonance. Their interpretation was confirmed by experiments and calculations on the vapor phase of the transition metals.[11-14] A thorough analysis of the Ni-metal loss data has been given by Dietz, McRae, and Weaver.[15]

Penn[16] has discussed resonant photoemission for a Hubbard model of the d bands in Ni. He has shown that the 6-eV satellite corresponds to a two-hole bound state, i.e., the d^8 configuration (also see Refs. 17–19). It is clear that much of the enhancement at resonance should occur in the satellite, since the SCK decay process preferentially goes to d^8 final states.[20] In Sec. IV, we consider the line shape and the intensity of both the satellite and the band emission. Recently, Yafet[21] has shown, in this regard, that different final states can have different resonant behavior (different Fano parameters q).

Iwan, Himpsel, and Eastman[22] found a similar but weaker resonance in Cu. This was unexpected since the Cu d bands are nominally full (actually 0.4 hole is present due to s-d hybridization) and the Penn mechanism requires some holes in the d bands. Iwan *et al.* suggested that a quasiatomic shakeup state involving the $3d^8$ configuration plus a low-lying nl electron (mainly $4s$) is responsible: $3p^6 3d^{10} 4s + h\nu \rightarrow 3p^5 3d^{10} 4snl \rightarrow 3p^6 3d^8 4snl \epsilon f$. This idea was also described by Wendin.[23] Such an explanation can only be regarded as qualitative, since it is inaccurate to treat $4s$-$4p$ electrons in Cu in an atomic manner. A solid-state model has been given by Davis and Feldkamp[24] and is discussed further in Sec. V. Girvin and Penn[25] have analyzed this model using perturbation theory.

Resonant photoemission has also been reported in Cr (Ref. 26), Zn (Ref. 27), Ga (Ref. 28), GaP (Ref. 28), NiO (Ref. 29), Ni-phthalocyanine (Ref. 30), and Cu-phthalocyanine (Ref. 31). All of these involve $3p$ core levels and the $3d$ valence electrons. (Here we do not consider materials in which the resonances involve other levels such as $4d$, $4f$, etc.)

The purpose of this paper is to extend the theory of the interaction of discrete states with many continua[32] to photoemission and to apply the formalism

to models which illustrate various aspects of resonant photoemission. In Sec. II, we present the general formalism. Intrinsic to this theory is treatment of the entire process as a coherent entity rather than separate, sequential processes of absorption and Auger decay. Our results overlap those of Yafet[21] and Wendin,[33] but are more general and use a different approach. In Sec. III, we consider a simple band model which exhibits both Auger and resonant emission features, but no satellite, similar to Cr. To our knowledge, this is the first time a Fano resonance has been discussed for a model in which no atomiclike effects (satellites, localized excitations, strong hole-hole interactions, etc.) are included. A model representing Ni which has a satellite and is rather atomiclike is given in Sec. IV. For metals with filled d bands [Cu (except for the effects of hybridization), Zn, etc.], the model discussed in Sec. V is applicable. Conclusions and further discussion are in Sec. VI.

II. FORMAL THEORY

Here we extend the formal theory of Ref. 32 to the calculation of the photoemission. We use the notation of Ref. 32 and consider a system with Hamiltonian $\hat{H}$ which has discrete basis functions ϕ_n and continuum basis functions ψ_{kE}. The interaction between ϕ_n and ψ_{kE} is described by

$$V_{kn}(E) = \langle \psi_{kE} | H | \phi_n \rangle . \tag{2.1}$$

In our applications, V_{kn} represents the SCK matrix element. As $r \to \infty$ (r is the coordinate of the photoelectron), ψ_{kE} has the form

$$\psi_{kE} = \Phi_k \sin[\kappa_k(E) r + \theta_k(E)]/r , \tag{2.2}$$

where Φ_k depends upon the spin σ and direction Ω of the photoelectron as well as the coordinates of the remaining electrons. Φ_k is a product, or linear combination of products, of a spherical harmonic $Y_{lm}(\Omega)$, a spin function χ_σ, and an eigenfunction (energy E_k') of the ionized system. Hence

$$\hbar^2 \kappa_k^2(E)/2m = E - E_k' . \tag{2.3}$$

The normalization is such that

$$\int d\Omega \langle \Phi_k | \Phi_{k'}' \rangle = \delta_{kk'} 2m/\pi\hbar^2\kappa_k , \tag{2.4}$$

and

$$\langle \psi_{k'E'} | \psi_{kE} \rangle = \delta_{kk'} \delta(E - E') . \tag{2.5}$$

We consider only the case where the number of discrete states N is less than or equal to the number of continua K. When V_{kn} is taken into account, the eigenfunctions of $\hat{H}$ are

$$\Psi_E^{(\nu)} = C_\nu(E) \sum_{n=1}^{N} A_n^{(\nu)}(E) \left(\bar{\phi}_n(E) + z_\nu(E) \sum_{k=1}^{K} V_{kn}(E) \psi_{kE} \right) , \quad \nu = 1, 2, \ldots, N \tag{2.6}$$

where

$$\bar{\phi}_n(E) = \phi_n + \sum_{k=1}^{K} \mathrm{P} \int \frac{dE'}{E - E'} V_{kn}(E') \psi_{kE'} , \tag{2.7}$$

$$z_\nu(E) = [\pi/\Gamma_\nu(E)][E - \bar{E}_\nu(E)] , \tag{2.8}$$

and

$$C_\nu(E) = [\pi/\Gamma_\nu(E)]^{1/2} [\pi^2 + z_\nu^2(E)]^{-1/2} . \tag{2.9}$$

$A_n^{(\nu)}(E)$ is the nth component of the νth eigenvector defined in Ref. 32 and

$$\pi \sum_{k=1}^{K} \bar{V}_{k\nu'}^*(E) \bar{V}_{k\nu}(E) = \Gamma_\nu(E) \delta_{\nu\nu'} , \tag{2.10}$$

where

$$\bar{V}_{k\nu}(E) = \sum_{n=1}^{N} A_n^{(\nu)}(E) V_{kn}(E) . \tag{2.11}$$

The "shifted resonance" energy $\bar{E}_\nu$ is given in Ref. 32. For $K > N$, there are $K - N$ solutions

$$\Psi_E^{(i)} = \sum_{k=1}^{K} \eta_k^{(i)}(E) \psi_{kE} , \quad i = N+1, \ldots, K \tag{2.12}$$

where

$$\sum_{k=1}^{K} \bar{V}_{k\nu}^*(E) \eta_k^{(i)}(E) = 0 , \quad \nu = 1, 2, \ldots, N \tag{2.13a}$$

and

$$\sum_{k=1}^{K} \eta_k^{(i')*}(E) \eta_k^{(i)}(E) = \delta_{ii'} . \tag{2.13b}$$

The photon field is described by

$$H_1(t) = T \exp(-i\omega t) + \mathrm{H.c.} \tag{2.14}$$

Here we define the energy of the ground state Φ_g as zero so that the wave function $\Psi(t)$ of the system [with Hamiltonian $= \hat{H} + H_1(t)$] is (to first order in T)

$$\Psi(t) = \Phi_g + \sum_{i=1}^{K} \int dE\, B_i(E, t) \Psi_E^{(i)} \exp(-iEt/\hbar) , \tag{2.15}$$

where

$$B_i(E,t) = -\frac{i}{\hbar} \int_0^t dt' \langle \Psi_E^{(i)} | H_1(t') | \Phi_g \rangle \exp(iEt'/\hbar) \tag{2.16}$$

$$= -\langle \Psi_E^{(i)} | T | \Phi_g \rangle \{ \exp[i(E - \hbar\omega)t/\hbar] - 1 \}/(E - \hbar\omega) . \tag{2.17}$$

In (2.17), the term involving $T^\dagger \exp(i\omega t)$ has been omitted since it does not contribute to the photocurrent.

We wish to calculate the flux of photoelectrons at $r \to \infty$. From (2.7) and (2.2), we find that

$$\bar{\phi}_n \to -\pi \sum_{k=1}^{K} V_{kn}(E)\Phi_k \cos[\kappa_k(E)r + \theta_k(E)]/r . \tag{2.18}$$

To find the behavior of $\Psi(t)$ as $r \to \infty$, we make use of the relationships [for $t/\hbar > \kappa'(\hbar\omega)r + \theta'(\hbar\omega)$]

$$\int dE \{\exp[i(E-\hbar\omega)t/\hbar] - 1\} \exp(-iEt/\hbar) \times \begin{Bmatrix} \cos \\ \sin \end{Bmatrix} [\kappa(E)r + \theta(E)]/(E-\hbar\omega)$$
$$= \pi \begin{Bmatrix} i \\ 1 \end{Bmatrix} \exp[-i\omega t + i\kappa(\hbar\omega)r + i\theta(\hbar\omega)] . \tag{2.19}$$

Setting $E = \hbar\omega$ we find from (2.6), (2.7), (2.11), (2.15), and (2.17)–(2.19)

$$\Psi(t) \to e^{-i\omega t} \sum_{k=1}^{K} D_k(E)\psi_{kE}^{(+)} , \tag{2.20}$$

where

$$D_k(E) = -\pi\left(\sum_{\nu=1}^{N} \langle \Psi_E^{(\nu)} | T | \Phi_g \rangle C_\nu(E)[-i\pi + z_\nu(E)]\overline{V}_{k\nu}(E) + \sum_{i=N+1}^{K} \langle \Psi_E^{(i)} | T | \Phi_g \rangle \eta_k^{(i)}(E) \right) \tag{2.21}$$

and

$$\psi_{kE}^{(+)} = \Phi_k \exp[i\kappa_k(E)r + i\theta_k(E)]/r . \tag{2.22}$$

The photoelectron flux (integrated over Ω) at $r \to \infty$ with kinetic energy $\epsilon = \hbar^2\kappa_k^2/2m$ in the kth channel is

$$N_k(E) = \frac{2}{\pi\hbar} |D_k(E)|^2 . \tag{2.23}$$

The photoelectron distribution is [see Eq. (2.3)]

$$N(E,\epsilon) = \sum_{k=1}^{K} N_k(E)\delta(\epsilon + E_k' - E) . \tag{2.24}$$

Using (2.10), (2.13), and (2.21), it can readily be shown that

$$\int d\epsilon\, N(E,\epsilon) = \frac{2}{\pi\hbar} \sum_{k=1}^{K} |D_k(E)|^2 \tag{2.25a}$$
$$= W(E) , \tag{2.25b}$$

where $W(E)$ is the rate of absorption of photons:

$$W(E) = \frac{2\pi}{\hbar}\left(\sum_{\nu=1}^{N} |\langle \Psi_E^{(\nu)} | T | \Phi_g \rangle|^2 + \sum_{i=N+1}^{K} |\langle \Psi_E^{(i)} | T | \Phi_g \rangle|^2 \right) . \tag{2.26}$$

Equation (2.26) expresses the rule that for each photon absorbed, a photoelectron is emitted.[21] This is a consequence of omitting radiative decay channels—a good approximation for the applications of interest here.

We can evaluate $D_k(E)$ by substituting (2.6) and (2.12) into (2.21) and using (2.9) and (2.11):

$$D_k(E) = -\pi \sum_{\nu=1}^{N} \frac{\pi}{\Gamma_\nu} (z_\nu + i\pi)^{-1}\overline{V}_{k\nu}\left(\sum_{n=1}^{N} A_n^{(\nu)*} \langle \bar{\phi}_n | T | \Phi_g \rangle + z_\nu \sum_{k'=1}^{K} \overline{V}_{k'\nu}^* \langle \psi_{k'E} | T | \Phi_g \rangle \right) - \pi \sum_{i=N+1}^{K} \eta_k^{(i)} \sum_{k'=1}^{K} \eta_{k'}^{(i)*} \langle \psi_{k'E} | T | \Phi_g \rangle . \tag{2.27}$$

[If $K = N$, the last term of (2.27) is omitted.] From (2.10) and (2.13) we note that the K vectors whose kth components are given by $\xi_k^{(\nu)} = \overline{V}_{k\nu}(\pi/\Gamma_\nu)^{1/2}$, $\nu = 1, 2, \ldots, N$ and $\eta_k^{(i)}$, $i = N+1, \ldots, K$, are orthonormal. Consequently we have

$$\sum_{i=N+1}^{K} \eta_k^{(i)}\eta_{k'}^{(i)*} = \delta_{kk'} - \pi \sum_{\nu=1}^{N} \overline{V}_{k\nu}\overline{V}_{k'\nu}^*/\Gamma_\nu . \tag{2.28}$$

Substituting (2.28) into (2.27) gives

$$D_k(E) = -\pi \langle \psi_{kE} | T | \Phi_g \rangle - \pi \sum_{\nu=1}^{N} [\pi \overline{V}_{k\nu}(E)/\Gamma_\nu(E)][z_\nu(E) + i\pi]^{-1} \times \left(\sum_{n=1}^{N} A_n^{(\nu)*}(E) \langle \bar{\phi}_n(E) | T | \Phi_g \rangle - i\pi \sum_{k'=1}^{K} \overline{V}_{k'\nu}^*(E) \langle \psi_{k'E} | T | \Phi_g \rangle \right) . \tag{2.29}$$

Provided the denominator is nonzero, it is useful to define a parameter[32]

$$q_\nu(E) = \sum_{n=1}^{N} A_n^{(\nu)}(E) \langle \Phi_g | T | \bar{\phi}_n(E) \rangle \left(\pi \sum_{k'=1}^{K} \overline{V}_{k'\nu}(E) \langle \Phi_g | T | \psi_{k'E} \rangle \right)^{-1} , \tag{2.30}$$

which we always take to be a real quantity. Using (2.30) in (2.29) gives

$$D_k(E) = -\pi \langle \psi_{kE} | T | \Phi_g \rangle - \pi \sum_{\nu=1}^{N} \left(\frac{\pi \overline{V}_{k\nu}(E)}{\Gamma_\nu(E)} \right) [z_\nu(E) + i\pi]^{-1} [q_\nu(E) - i]\pi \sum_{k'=1}^{K} \overline{V}_{k'\nu}^*(E) \langle \psi_{k'E} | T | \Phi_g \rangle . \tag{2.31}$$

From (2.25), we can show that

$$W(E)=\frac{2\pi}{\hbar}\left\{\sum_{k=1}^{K}|\langle\psi_{kE}|T|\Phi_g\rangle|^2-\sum_{\nu=1}^{N}[\pi/\Gamma_\nu(E)]\left|\sum_{k=1}^{K}\overline{V}^*_{k\nu}(E)\langle\psi_{kE}|T|\Phi_g\rangle\right|^2\right.$$
$$\left.+\sum_{\nu=1}^{N}[\pi/\Gamma_\nu(E)]\left|\sum_{k=1}^{K}\overline{V}^*_{k\nu}(E)\langle\psi_{kE}|T|\Phi_g\rangle\right|^2[q_\nu(E)+z_\nu(E)/\pi]^2/\{[z_\nu(E)/\pi]^2+1\}\right\}. \quad (2.32)$$

The last term of (2.32) is the "resonant" part of the absorption and the first two terms represent "background." [When $K=N$, $W(E)$ contains only the resonant term.]

As pointed out by Yafet[21] and independently by Wendin,[33] the energy dependence of $N_k(E)$ is, in general, different from that of $W(E)$; that is, the intensity of emission corresponding to a given final state k does not depend upon photon energy $E=h\nu=\hbar\omega$ near resonance in the same manner as the absorption.

At this point it is worthwhile to explore the meaning of the sum rule (2.25) as it applies to solids and the relationship of $W(E)$ to the absorption coefficient and the macroscopic electric field. If we exclude secondary electrons and regard the surface electron transmission as a constant (independent of E), the total number of photoelectrons must be proportional to the number of photons absorbed in a region near the surface whose width is λ_{ee}, the electron escape depth. This is the sense of (2.25). Omitting surface photoemission (e.g., from surface states), we find the total electron photoemission for a surface area A to be

$$W_{\lambda_{ee}}(E)=\text{const}\times\text{Im}[\epsilon(\omega)]|\vec{\mathrm{E}}|^2\lambda_{ee}A/2\pi\hbar \quad (2.33)$$
$$=\text{const}\times nc\mu|\vec{\mathrm{E}}|^2\lambda_{ee}A/2\pi\hbar \quad (2.34)$$

where $\epsilon(\omega)$ is the dielectric constant, $n=\text{Re}\epsilon(\omega)^{1/2}$, $\vec{\mathrm{E}}\exp(-i\omega t)+\text{c.c.}$ is the macroscopic electric field just inside the surface of the solid, and μ is the absorption coefficient. Although it is customary to compare integrated yield to μ under conditions of constant incident flux, there is some ω dependence in the factor $n|\vec{\mathrm{E}}|^2/\omega$ as well as in the transmission factor and λ_{ee}. (Here we assume that $\mu\lambda_{ee}\ll1$.) In Ref. 32, we called attention to the differences in line shapes among similar quantities, $\text{Im}\epsilon$, $\text{Im}(-1/\epsilon)$, μ, etc. The ω dependence of the factor $n|\vec{\mathrm{E}}|^2/\omega$ could well introduce such differences between μ and the yield.

If we use a single-particle or an atomic description, the interaction operator T involves the macroscopic field (as opposed to the applied field) inside the solid. Hence

$$T=\sum_j T_j, \quad (2.35)$$

where

$$T_j=(e/im\omega)\vec{\mathrm{E}}\cdot\vec{\mathrm{p}}_j \quad (2.36a)$$

or

$$T_j=e\vec{\mathrm{x}}_j\cdot\vec{\mathrm{E}}. \quad (2.36b)$$

the sum being over all the electrons in the system. Substituting (2.36) into (2.26) gives

$$W(E)=\frac{2\pi}{\hbar}\frac{e^2}{m^2\omega^2}|\vec{\mathrm{E}}|^2\sum_{i=1}^{K}\left|\left\langle\Psi_E^{(i)}\right|\sum_j\hat{e}\cdot\vec{\mathrm{p}}_j\left|\Phi_g\right\rangle\right|^2 \quad (2.37a)$$

$$=\frac{2\pi}{\hbar}e^2|\vec{\mathrm{E}}|^2\sum_{i=1}^{K}\left|\left\langle\Psi_E^{(i)}\right|\sum_j\hat{e}\cdot\vec{\mathrm{x}}_j\left|\Phi_g\right\rangle\right|^2 \quad (2.37b)$$

$$=\text{Im}\epsilon(\omega)|\vec{\mathrm{E}}|^2V/2\pi\hbar, \quad (2.38)$$

where $\hat{e}$ is the polarization vector ($\vec{\mathrm{E}}=|\vec{\mathrm{E}}|\hat{e}$) and V is the system volume. Although we calculate the absorption for the entire volume of the sample, it is only a small region near the surface which actually contributes to the measured photocurrents ($V\sim A\lambda_{ee}$). Consequently, we neglect the variation of $\vec{\mathrm{E}}$ with position. For simplicity, we use the length form (2.36b) and take $|\vec{\mathrm{E}}|^2$ to be independent of ω in the model calculations of Secs. III–V. Clearly the results could be multiplied by a factor which varies slowly with frequency without affecting the results significantly.

III. APPLICATION TO Cr

A. Description of model

Resonant photoemission involving SCK transitions is generally associated with atomiclike effects. For example, strong $3d$ hole-hole interaction results in localized excitations, so that Ni can be treated from a purely atomic point of view in first approximation.[3] However, it would be incorrect to assume that a Fano resonance cannot occur in a purely band model (single-particle picture) in which no electron-electron interactions are present. Such considerations are important because Cr metal neither has a satellite in x-ray photoemission spectroscopy nor does the $L_{2,3}M_{4,5}M_{4,5}$ Auger spectrum[34] appear atomiclike as in Ni, but nonetheless the valence-band emission shows a strong dip near the $3p$ threshold.[25] In this section, we investigate Fano resonances in a simple band model.

Let us consider a paramagnetic solid consisting of N_0 atoms. (The fact that Cr is actually antiferromagnetic is of no consequence here.) The discrete excited states are

$$\phi_n = c^\dagger_{p\sigma} b_s |\Phi_g\rangle , \tag{3.1}$$

where $c^\dagger_{p\sigma}$ creates an electron in an empty band state p (energy $= \epsilon_p$, p = wave vector and band index) with spin σ and b_s creates a hole with spin s in a core level at the origin (energy $= \epsilon_c$). The energy is

$$E_n = \epsilon_p - \epsilon_c . \tag{3.2}$$

The number of such states is $N_B N_0$ (for a given s).

The continuum states are of two types. The first type gives rise to interference (coherent processes) and will be designated by I:

$$\psi^{(I)}_{kE} = a^\dagger_{\epsilon l m_s} c_{p'\sigma'} |\Phi_g\rangle , \tag{3.3}$$

where $a^\dagger_{\epsilon l m_s}$ creates an electron in the ϵl continuum orbital (here l stands for all orbital quantum numbers) with spin m_s and $p'\sigma'$ is a valence electron (occupied state). There are $N_V N_0$ continuum states for each $l m_s$. The energy is

$$E = \epsilon - \epsilon_{p'} . \tag{3.4}$$

The other type of continuum state gives rise to Auger excitations (incoherent) and will be designated by A:

$$\psi^{(A)}_{kE} = a^\dagger_{\epsilon l m_s} c^\dagger_{\tilde{p}\tilde{\sigma}} c_{p_1\sigma_1} c_{p_2\sigma_2} |\Phi_g\rangle , \tag{3.5}$$

where

$$E = \epsilon + \epsilon_{\tilde{p}} - \epsilon_{p_1} - \epsilon_{p_2} . \tag{3.6}$$

We take the matrix elements to be of the form

$$V^{(I)}_{kn}(E) = -\frac{V_I}{N_0} (\delta_{s\sigma'} \delta_{m_s\sigma} - \delta_{s\sigma} \delta_{m_s\sigma'}) \tag{3.7}$$

and

$$V^{(A)}_{kn}(E) = -\frac{V_I}{N_0} (\delta_{\sigma_1 s} \delta_{\sigma_2 m_s} - \delta_{\sigma_1 m_s} \delta_{\sigma_2 s}) \delta_{\tilde{p}p} \delta_{\tilde{\sigma}\sigma} . \tag{3.8}$$

That is, we neglect the dependence upon p, p', p_1, and p_2.

To find the solutions $z_\nu(E)$ and $A^{(\nu)}_n$ required in Sec. II, we must solve[32]

$$(E_n - E) A_n(E) + \sum_m F_{nm}(E) A_m(E) + [z(E)/\pi] \sum_m \Gamma_{nm}(E) A_m(E) = 0 , \tag{3.9}$$

where

$$F_{nm}(E) = \frac{1}{\pi} \mathrm{P} \int \Gamma_{nm}(E') dE' / (E - E') , \tag{3.10}$$

and

$$\Gamma_{nm}(E) = \pi \sum_k V^*_{kn}(E) V_{km}(E) , \tag{3.11}$$

with

$$\sum_n |A^{(\nu)}_n(E)|^2 = 1 . \tag{3.12}$$

From (3.7), (3.8), and (3.11), we find ($n = p\sigma s$ and $m = \bar{p}\bar{\sigma}\bar{s}$)

$$\Gamma_{nm} = [(\Gamma_I/N_0) + \Gamma_c \delta_{p\bar{p}}] \delta_{\sigma\bar{\sigma}} \delta_{s\bar{s}} , \tag{3.13}$$

where

$$\Gamma_I = (N_v/2)\Gamma_0 , \tag{3.14}$$

$$\Gamma_c = (N_v/2)^2 \Gamma_0 , \tag{3.15}$$

and

$$\Gamma_0 = \pi \sum_l V_l^2 . \tag{3.16}$$

It can be shown that $2\Gamma_c$ is the x-ray photoelectron spectrum width [full width at half maximum (FWHM)] of the core level. Here we assume that the empty states are in the same bands as the valence electrons (3d bands in our examples).

Equation (3.13) indicates an interesting feature of the band model. As might be expected, the interference term in the diagonal matrix element is of order $1/N_0$. Although it is tempting to neglect it as well as the off-diagonal terms since N_0 is large, explicit calculation shows this to be wrong. Such neglect would amount to omitting all interference effects (which are of order 1, not $1/N_0$).

Only solutions where $\sigma = s$ are of interest, since absorption does not change the spin. Without loss of generality we take $\sigma = s = \uparrow$, since spin $\downarrow$ will be identical. Then the label n becomes just p (m becomes $\bar{p}$) and (3.9) reads [using (3.2), (3.10), and (3.13)–(3.15)]

$$(\epsilon_p - \epsilon_c - E + F_c) A_p + \frac{F_I}{N_0} \sum_{\tilde{p}} A_{\tilde{p}} + \frac{z(E)}{\pi} \Gamma_c A_p + \frac{z(E)}{\pi} \frac{\Gamma_I}{N_0} \sum_{\tilde{p}} A_{\tilde{p}} = 0 , \tag{3.17}$$

where

$$F_{I,c}(E) = \frac{1}{\pi} \mathrm{P} \int \Gamma_{I,c}(E') dE' / (E - E') . \tag{3.18}$$

The sum on $\bar{p}$ is over empty states (one spin only).

It is expedient to assume that all ϵ_p are nondegenerate. Then it is straightforward to show that the solutions to (3.17) are given by the solutions $z = z_\nu(E)$ of

$$\Lambda(E, z) = F_I + (z/\pi)\Gamma_I , \tag{3.19}$$

where

$$\Lambda^{-1}(E, z) = \frac{1}{N_0} \sum_p \frac{1}{E - \epsilon_p + \epsilon_c - F_c - (z/\pi)\Gamma_c} . \tag{3.20}$$

The corresponding eigenvector is

$$A_p^{(\nu)}(E)=\xi_p(E,z_\nu(E))\Big/\left(\sum_p \xi_p^2(E,z_\nu(E))\right)^{1/2}, \tag{3.21}$$

where

$$\xi_p(E,z)=\frac{1}{\sqrt{N_0}}\frac{\Lambda(E,z)}{E-\epsilon_p+\epsilon_c-F_c-(z/\pi)\Gamma_c}. \tag{3.22}$$

Furthermore, we find from (2.11), (3.7), and (3.8) for $\sigma=s=\uparrow$

$$\overline{V}_{k\nu}^{(I)}=\frac{V_l}{N_0}\sum_p A_p^{(\nu)}\delta_{m_s\downarrow}\delta_{\sigma'\downarrow} \tag{3.23}$$

for any p' and

$$\overline{V}_{k\nu}^{(A)}=\frac{V_l}{N_0}A_{\tilde{p}}^{(\nu)}\delta_{\tilde{\sigma}\uparrow}\delta_{m_s\downarrow} \tag{3.24}$$

for any p_1 and p_2. In (3.23), the matrix elements for $m_s=\sigma'=\uparrow$ (with $\sigma=s=\uparrow$) vanish since the direct and exchange Auger terms cancel. In (3.24) we take $\sigma_1=\downarrow$ and $\sigma_2=\uparrow$ to avoid double counting. From (2.10), (3.23), and (3.24), we have

$$\Gamma_\nu=\frac{\Gamma_I}{N_0}\left(\sum_p A_p^{(\nu)}\right)^2+\Gamma_c. \tag{3.25}$$

The dipole matrix elements are

$$\langle\psi_{kE}^{(I)}|T|\Phi_g\rangle=\langle\epsilon l|T|p'\rangle \tag{3.26}$$

and

$$\langle\psi_{kE}^{(A)}|T|\Phi_g\rangle=0. \tag{3.27}$$

Equation (3.27) holds because $\psi_{kE}^{(A)}$ can not be reached from Φ_g by a single-particle excitation.

It can be shown from (2.30) and (3.1) that

$$q_\nu=q=t_0\Big/\left(\pi\sum_l V_l t_l\right), \tag{3.28}$$

where the core level to p matrix element is independent of p:

$$\langle p|T|\text{core}\rangle=t_0'/\sqrt{N_0}, \tag{3.29}$$

$$t_0=t_0'+\sum_l \mathrm{P}\int\frac{dE'}{E-E'}V_l(E')t_l(E'), \tag{3.30}$$

and

$$t_l(E)=\frac{1}{\sqrt{N_0}}\sum_{p'}\langle\epsilon l|T|p'\rangle. \tag{3.31}$$

In evaluating (2.31), we encounter sums (for fixed E) which are conveniently expressed in terms of an integral:

$$\sum_\nu\frac{F(z_\nu)}{\Gamma_I+\Gamma_c\sum_{\tilde{p}}\xi_{\tilde{p}}^2(E,z_\nu)}=\frac{1}{2\pi i}\oint_C\frac{dz\,F(z)}{\pi h(E,z)}, \tag{3.32}$$

where $F(z)$ is analytic on and near the real axis, the contour C encloses the poles $z_\nu(E)$ on the real axis, and

$$h(E,z)=(z/\pi)\Gamma_I+F_I-\Lambda(E,z). \tag{3.33}$$

Consequently,

$$D_k^{(I)}(E)=-\pi\left[\langle\epsilon l|T|p'\rangle+\frac{\pi^2V_l}{\sqrt{N_0}}\left(\sum_{l'}V_{l'}t_{l'}\right)(q-i)\times\frac{1}{2\pi i}\oint_C\frac{dz}{\pi h(E,z)}\frac{1}{z+i\pi}\right]. \tag{3.34}$$

By deforming the contour,

$$\frac{1}{2\pi i}\oint\frac{dz}{\pi h(E,z)}\frac{1}{z+i\pi}=\frac{-1}{\pi h(E,-i\pi)}. \tag{3.35}$$

From (3.33), we have

$$h(E,-i\pi)=F_I-i\Gamma_I-\Lambda(E,-i\pi), \tag{3.36}$$

where, using (3.20),

$$\Lambda^{-1}(E,-i\pi)=\int\frac{d\mathcal{E}\,\rho_B(\mathcal{E})}{E-\mathcal{E}+\epsilon_c-F_c+i\Gamma_c} \tag{3.37}$$

and

$$\rho_B(\mathcal{E})=\frac{1}{N_0}\sum_p\delta(\mathcal{E}-\epsilon_p) \tag{3.38}$$

is the density of empty states per site for one spin. Note that $\int d\mathcal{E}\,\rho_B(\mathcal{E})=N_B/2$. A similar calculation gives

$$D_k^{(A)}(E)=\pi^2V_l\left(\sum_{l'}V_{l'}t_{l'}\right)\frac{q-i}{N_0^{3/2}}\frac{\Lambda(E,-i\pi)}{h(E,-i\pi)}\times\frac{1}{E-\epsilon_{\tilde{p}}+\epsilon_c-F_c+i\Gamma_c}. \tag{3.39}$$

The photoemission intensity for the interference or coherent processes is (both spins)

$$N^{(I)}(E,\epsilon)=\frac{4}{\pi\hbar}\sum_{p'}|D_k^{(I)}(E)|^2\delta(E-\epsilon+\epsilon_{p'}). \tag{3.40}$$

If we replace $\sum_l|\langle\epsilon l|T|p'\rangle|^2$ by its average, $(2/N_V)\sum_l t_l^2$, then from (3.34) and (3.40)

$$N^{(I)}(E,\epsilon)=\frac{2\pi}{\hbar}N_0 2\rho_V(\epsilon-E)\left[\frac{2}{N_V}\sum_l t_l^2-2\pi\frac{N_c}{N_V}\left(\sum_l V_l t_l\right)^2\mathrm{Re}\left(\frac{q-i}{h(E,-i\pi)}\right)+\pi^2\frac{N_0}{2}\left(\sum_l V_l^2\right)\left(\sum_l V_l t_l\right)^2\frac{q^2+1}{|h(E,-i\pi)|^2}\right], \tag{3.41}$$

where

$$\rho_V(\mathcal{E})=\frac{1}{N_0}\sum_p\delta(\mathcal{E}-\epsilon_{p'}) \tag{3.42}$$

is the density of filled states per site for one spin. Note $\int d\mathcal{E}\,\rho_V(\mathcal{E})=N_V/2$. In the second and third terms of (3.41) we have inserted a factor of $N_0N_c/2$ to account for the number of core levels (N_c per site counting both spins) and number of sites, since our development has considered only one core level at the origin.

Similarly, from (3.39) we have

$$N^{(A)}(E,\epsilon)=\frac{2\pi}{\hbar}N_0N_c\left(\frac{2}{N_V}\right)^2(q^2+1)\left(\pi\sum_l V_l t_l\right)^2 \times\int d\mathcal{E}\,\frac{\Gamma_c/\pi}{\mathcal{E}^2+\Gamma_c^2}S_{VV}(\mathcal{E}+\epsilon_c-F_c+\epsilon)\rho_B(\mathcal{E}+\epsilon_c-F_c+E)\left|\frac{\Lambda(E,-i\pi)}{h(E,-i\pi)}\right|^2, \tag{3.43}$$

where

$$S_{VV}(\mathcal{E})=\int d\mathcal{E}'\rho_V(\mathcal{E}')\rho_V(\mathcal{E}-\mathcal{E}') \tag{3.44}$$

is the self-convolution of the valence-band density of states. Note $\int d\mathcal{E}\,S_{VV}(\mathcal{E})=(N_V/2)^2$. The absorption, which is the sum of (3.41) and (3.43) integrated over ϵ (quantities such as V_l and t_l which vary slowly with ϵ are evaluated at an appropriate average value), is

$$W(E)=\frac{2\pi}{\hbar}N_0\left[2\sum_l t_l^2+\pi N_c\left(\sum_l V_l t_l\right)^2\mathrm{Im}[(q-i)^2/h(E,-i\pi)]\right]. \tag{3.45}$$

If we wish to include Auger transitions in which the core electron is absorbed into broad empty bands which cause no interference (e.g., the 4s-4p bands), the additional photoemission is given by

$$N^{(A)'}(E,\epsilon)=\frac{2\pi}{\hbar}N_0N_c\left(\frac{2}{N_V}\right)^2\int d\mathcal{E}\,\frac{\Gamma_c/\pi}{\mathcal{E}^2+\Gamma_c^2}S_{VV}(\mathcal{E}+\epsilon_c-F_c+\epsilon)\sum_\kappa|\langle\kappa|T|\text{core}\rangle|^2\delta(\mathcal{E}+\epsilon_c-F_c+E-\epsilon_\kappa). \tag{3.46}$$

Here we designate the empty band states by κ and keep a general form of dipole matrix element. The integral over of $N^{(A)'}(E,\epsilon)$ is to be added to (3.45). The principal difference between (3.43) and (3.46) is that for narrow 3d bands (for example) the intensity represented by $N^{(A)}(E,\epsilon)$ is confined to an interval in kinetic energy around $\epsilon\simeq E-\epsilon_F+2\langle\epsilon_{p'}\rangle$ for any E, where $\langle\epsilon_{p'}\rangle$ is the average energy of the filled states. On the other hand, the peak in $N^{(A)'}(E,\epsilon)$ occurs at $\epsilon\simeq 2\langle\epsilon_{p'}\rangle-\epsilon_c+F_c$ for E above threshold. The former is at fixed binding energy $(E-\epsilon)$ whereas the latter is at fixed kinetic energy as a function of E (photon energy).

B. Numerical results

We consider a simple density of states

$$\rho_B(\mathcal{E})=\begin{cases}\dfrac{N_B}{2W_B}, & \epsilon_F<\mathcal{E}<\epsilon_F+W\\ 0 \quad \text{otherwise}.\end{cases} \tag{3.47}$$

Defining

$$R_V=\frac{2\pi}{\hbar}N_0\,2\sum_l t_l^2, \tag{3.48}$$

which is the integrated photoemission intensity in the absence of resonance effects, we have from (3.41)

$$N^{(I)}(E)=\int d\epsilon\,N^{(I)}(E,\epsilon) \tag{3.49}$$

$$=R_V\{1+\tau N_c\,\mathrm{Re}[(q-i)J(E)] +(\tau/4)N_VN_c(q^2+1)|J(E)|^2\}, \tag{3.50}$$

where

$$\tau=\left(\sum_l V_l t_l\right)^2\Big/\left[\left(\sum_l V_l^2\right)\left(\sum_l t_l^2\right)\right], \tag{3.51}$$

$$J(E)=\frac{\Gamma_0N_B[L(E)-iT(E)]/2W_B}{1-(F_I-i\Gamma_I)N_B[L(E)-iT(E)]/2W_B}, \tag{3.52}$$

$$L(E)=\tfrac{1}{2}\ln\left(\frac{(E-E_{\text{th}})^2+\Gamma_c^2}{(E-E_{\text{th}}-W_B)^2+\Gamma_c^2}\right), \tag{3.53}$$

$$T(E)=\tan^{-1}[(E-E_{\text{th}})/\Gamma_c] +\tan^{-1}[(E_{\text{th}}-E+W_B)/\Gamma_c], \tag{3.54}$$

and

$$E_{\text{th}}=\epsilon_F-\epsilon_c+F_c. \tag{3.55}$$

From (3.43),

$$N^{(A)}(E)=\int d\epsilon\,N^{(A)}(E,\epsilon) \tag{3.56}$$

$$=R_V\frac{\tau(q^2+1)\Gamma_0N_BN_cT(E)/4W_B}{|1-(F_I-i\Gamma_I)N_B[L(E)-iT(E)]/2W_B|^2}. \tag{3.57}$$

In Fig. 1, we give results for parameters roughly typical of Cr. The interference term $N^{(I)}(E)$ (integrated coherent photoemission as a function of photon energy) shows a pronounced dip at threshold, whereas the absorption shows less dip because the Auger intensity $N^{(A)}(E)$ turns on in this region. The peak at $E-E_{\text{th}}=h\nu-h\nu_0=5$ eV is associated with the sharp cutoff of the density of

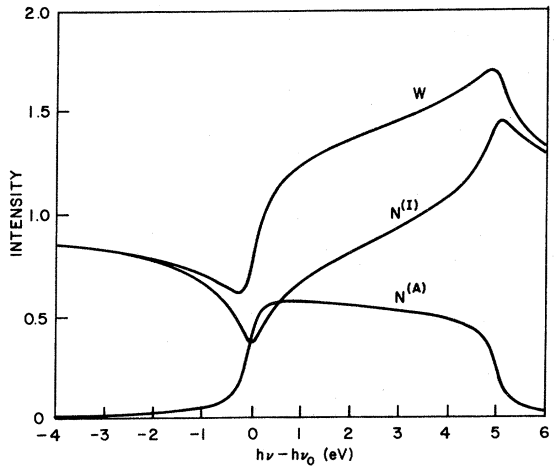

FIG. 1. Photoemission intensity (yield) and absorption in units of R_V vs photon energy for band model with parameters appropriate to Cr: $N_V=N_B=5$, $N_C=6$, $W_B=5$ eV, $\Gamma_0=0.03$ eV, $q=2$, $\tau=1$, and $F_I=-\Gamma_I$. $N^{(A)}(E)$ is the integrated photoemission due to Auger transitions and $N^{(I)}(E)$ to interference (coherent) processes. The absorption $W(E)=N^{(I)}(E)+N^{(A)}(E)$, $E=h\nu$, and $h\nu_0=E_{\rm th}$.

states at ϵ_F+W_B and would be smoothed out if $\rho_B(E)$ went to zero more gently. The sharp edge at ϵ_F is realistic because it represents the Fermi factor. We do not consider the additional Auger transitions $N^{(A)'}$.

For fixed photon energy, the spectrum $N^{(I)}(E,\epsilon)$ as a function of electron energy ϵ is given by the occupied valence-band density of states ρ_V. Likewise, the Auger term for fixed photon energy depends upon the self-convolution of ρ_V and lifetime broadening. For $\Gamma_c \ll h\nu - h\nu_0 \ll W - \Gamma_c$, the Auger term as a function of ϵ is approximately independent of $h\nu$ in this example, i.e., the Auger electron is at "fixed" kinetic energy.

The qualitative features of Fig. 1 are, in many respects, similar to the data for Cr.[26] In particular, the valence-band emission shows a large dip at threshold. We conclude that interference occurs in the yield and in the absorption.[5,9] The observed Auger peak corresponds to the decay following excitation of the $3p$ core electron to empty $3d$ bands as well as the $4s$-$4p$ and other bands.

In Ref. 8, we analyzed the Cr absorption in terms of atomic multiplet splittings. Here we omit such effects and concentrate on band effects. A more comprehensive model would include both aspects. Also, Barth *et al.*[26] discuss additional decay mechanisms not considered in the present work.

IV. APPLICATION TO Ni

A. Description of model

In this section, we present results for a model which represents the essential physics of the Ni-metal resonance. This model differs from that of Sec. III in that hole-hole (or hole-electron) interactions are included. Consequently, atomiclike effects, including the presence of a two-hole satellite in nonresonant photoemission, are specifically considered. We are interested in the difference in the $h\nu$ dependence of the main line and satellite spectra and in the effect of interference on the line shapes.

Let us consider a filled spin $\uparrow d$ band and a partially filled spin $\downarrow d$ band (neglecting the orbital degeneracy of the d bands). For simplicity, we neglect the dispersion (width) of the $\uparrow d$ band. Hence the model is the strongly ferromagnetic Hubbard model in which the $\uparrow$ band is flat. Strictly speaking, it applies to a transition of the type $2p \rightarrow 3d$ followed by $L_{2,3}M_{2,3}M_{4,5}$ decay, but here we apply it to $3p \rightarrow 3d$ followed by $M_{2,3}M_{4,5}M_{4,5}$ decay. The model is similar to, although not identical to, that considered by Penn.[16] Our analysis differs from Penn's and we examine different aspects.

In the presence of a $3p$ core hole, the $\downarrow$ electrons see a local potential $-V$ at the core site ($i=0$, for example).[18] (It is not necessary to include the interaction of the $\uparrow$ electrons with the core hole since it can be absorbed in the definition of excitation energies.) The Hamiltonian is

$$H=\sum_{\vec{k}}\epsilon_{\vec{k}\downarrow}d^\dagger_{\vec{k}\downarrow}d_{\vec{k}\downarrow}+\epsilon_{\uparrow}\sum_i d^\dagger_{i\uparrow}d_{i\uparrow}+U\sum_i n_{i\uparrow}n_{i\downarrow} - Vn_{i=0\downarrow}bb^\dagger+\epsilon_c b^\dagger b\,, \tag{4.1}$$

where $\epsilon_{\vec{k}\downarrow}$ is the orbital energy and $d^\dagger_{\vec{k}\downarrow}$ is the creation operator for the $\vec{k}\downarrow$ Bloch state, $\epsilon_{\uparrow}$ is the (average) energy of the $\uparrow$ band, U is the d-d electron-electron interaction (as in the Hubbard model), $b^\dagger$ creates a $\downarrow$ core electron,

$$n_{i\sigma}=d^\dagger_{i\sigma}d_{i\sigma}\,, \tag{4.2a}$$

and

$$d_{i\sigma}=N_0^{-1/2}\sum_{\vec{k}}\exp(i\vec{k}\cdot\vec{R}_i)d_{\vec{k}\sigma}\,. \tag{4.2b}$$

Let

$$|\Phi\rangle=b^\dagger\prod_{i=1}^{N_0}d^\dagger_{i\uparrow}|0\rangle \tag{4.3}$$

where $|0\rangle$ is the vacuum. The ground state is

$$|\Phi_g\rangle=\prod_{j=1}^{L}d_{\vec{k}_j\downarrow}|\Phi\rangle\,, \tag{4.4}$$

where $\vec{k}_1,\vec{k}_2,\ldots,\vec{k}_L$ are the L lowest energy $\downarrow$ orbitals. The ground state energy is

$$E_g=\sum_{j=1}^{L}\epsilon_{\vec{k}_j\downarrow}+\epsilon_c+LU+N_0\epsilon_{\uparrow}\,. \tag{4.5}$$

The discrete states (ϕ_n of Sec. II), corresponding

to the excitation of a core electron to the $\downarrow d$ band, are[18]

$$b\,|\Phi_\alpha\rangle = b\prod_{j=1}^{L+1} c^\dagger_{n_j}|\Phi\rangle \tag{4.6}$$

with energy

$$E_\alpha = \sum_{j=1}^{L+1}\omega_{n_j} + N_0\epsilon_\uparrow + (L+1)U\,, \tag{4.7}$$

where

$$d_{\vec{k}\downarrow} = \sum_n S_{\vec{k}n}c_n \tag{4.8}$$

and

$$(\epsilon_{\vec{k}\downarrow} - \omega_n)S_{\vec{k}n} = \frac{V}{N_0}\sum_{\vec{k}'} S_{\vec{k}'n}\,, \tag{4.9}$$

so that

$$\sum_{\vec{k}}\epsilon_{\vec{k}\downarrow}d^\dagger_{\vec{k}\downarrow}d_{\vec{k}\downarrow} - Vn_{i=0\downarrow} = \sum_n \omega_n c^\dagger_n c_n\,. \tag{4.10}$$

The index α stands for $\{n_1, n_2, \ldots, n_{L+1}\}$.

The continua (ψ_{kE} of Sec. II), corresponding to the photoionization of a $\downarrow d$ electron, are

$$a^\dagger_{\epsilon l\downarrow}d_{i=0\downarrow}|\Phi'_\beta\rangle = a^\dagger_{\epsilon l\downarrow}d_{i=0\downarrow}\prod_{j=1}^{L} c'^\dagger_{m_j}|\Phi\rangle \tag{4.11}$$

where $a^\dagger_{\epsilon l\downarrow}$ creates an $\epsilon l\downarrow$ continuum electron, $\beta = \{m_1, m_2, \ldots, m_L\}$, and c'_m is analogous to c_n with V replaced by U in (4.9) and (4.10). The energy associated with (4.11) is

$$E = \epsilon + E'_\beta\,, \tag{4.12}$$

where

$$E'_\beta = \sum_{j=1}^{L}\omega_{m_j} + (N_0 - 1)\epsilon_\uparrow + LU + \epsilon_c\,. \tag{4.13}$$

The matrix element V_{kn} is, from (2.1), (4.6), and (4.11)

$$\langle\Phi'_\beta|d^\dagger_{i=0\downarrow}a_{\epsilon l\downarrow}\hat{H}b\,|\Phi_\alpha\rangle = -\langle p\epsilon l\,|e^2/r\,|dd\rangle\langle\Phi'_\beta|d_{i=0\downarrow}|\Phi_\alpha\rangle\,, \tag{4.14}$$

where $\langle p\epsilon l\,|e^2/r\,|dd\rangle$ is an atomiclike SCK matrix element. Note that in this section, p means $3p$ core. It is straightforward to show from (4.3), (4.6), (4.8), and (4.11) that

$$\langle\Phi'_\beta|d_{i=0\downarrow}|\Phi_\alpha\rangle = \begin{vmatrix} N_0^{-1/2}\sum_{\vec{k}} S_{\vec{k}n_1} & N_0^{-1/2}\sum_{\vec{k}} S_{\vec{k}n_2} & \cdots & N_0^{-1/2}\sum_{\vec{k}} S_{\vec{k}n_{L+1}} \\ \langle m_1|n_1\rangle & \langle m_1|n_2\rangle & \cdots & \langle m_1|n_{L+1}\rangle \\ \cdots & \cdots & \cdots & \cdots \\ \langle m_L|n_1\rangle & \langle m_L|n_2\rangle & \cdots & \langle m_L|n_{L+1}\rangle \end{vmatrix}, \tag{4.15}$$

where

$$\langle m\,|n\rangle = \sum_{\vec{k}} S'^*_{\vec{k}m}S_{\vec{k}n}\,. \tag{4.16}$$

$S'_{\vec{k}m}$ is analogous to $S_{\vec{k}n}$ with V replaced by U in (4.9).

The dipole matrix element to a continuum state is

$$\langle\psi_{kE}|\,T\,|\Phi_g\rangle = \langle\epsilon l\,|T\,|d\rangle\langle\Phi'_\beta|\,\Phi_g\rangle\,, \tag{4.17}$$

where $\langle\epsilon l\,|T\,|d\rangle$ is atomiclike and[18]

$$\langle\Phi'_\beta|\,\Phi_g\rangle = \begin{vmatrix} S'^*_{\vec{k}_1m_1} & S'^*_{\vec{k}_1m_2} & \cdots & S'^*_{\vec{k}_1m_L} \\ S'^*_{\vec{k}_2m_1} & S'^*_{\vec{k}_2m_2} & \cdots & S'^*_{\vec{k}_2m_L} \\ \cdots & \cdots & \cdots & \cdots \\ S'^*_{\vec{k}_Lm_1} & S'^*_{\vec{k}_Lm_2} & \cdots & S'^*_{\vec{k}_Lm_L} \end{vmatrix} \tag{4.18}$$

The dipole matrix element to a discrete state is

$$\langle\phi_n|\,T\,|\Phi_g\rangle = -\langle d\,|T\,|p\rangle\langle\Phi_\alpha|d^\dagger_{i=0\downarrow}|\Phi_g\rangle\,, \tag{4.19}$$

where $\langle d\,|T\,|p\rangle$ is atomiclike and

$$\langle\Phi_\alpha|d^\dagger_{i=0\downarrow}|\Phi_g\rangle = \begin{vmatrix} N_0^{-1/2}\sum_{\vec{k}} S^*_{\vec{k}n_1} & N_0^{-1/2}\sum_{\vec{k}} S^*_{\vec{k}n_2} & \cdots & N_0^{-1/2}\sum_{\vec{k}} S^*_{\vec{k}n_{L+1}} \\ S^*_{\vec{k}_1n_1} & S^*_{\vec{k}_1n_2} & \cdots & S^*_{\vec{k}_1n_{L+1}} \\ \cdots & \cdots & \cdots & \cdots \\ S^*_{\vec{k}_Ln_1} & S^*_{\vec{k}_Ln_2} & \cdots & S^*_{\vec{k}_Ln_{L+1}} \end{vmatrix}. \tag{4.20}$$

The matrix element of Γ (in the ϕ_n representation) is, from Eq. (15) of Ref. 32 and (4.14),

$$\Gamma_{\alpha'\alpha} = \Gamma_0 \langle \Phi_{\alpha'} | n_{i=0\downarrow} | \Phi_\alpha \rangle \tag{4.21}$$

where the SCK width ($2\Gamma_0$ = FWHM) is

$$\Gamma_0 = \pi \sum_l |\langle p\epsilon l | e^2/r | dd \rangle|^2 . \tag{4.22}$$

In what follows we require only the diagonal terms of Γ so we note that

$$\langle \Phi_\alpha | n_{i=0\downarrow} | \Phi_\alpha \rangle = N_0^{-1} \sum_{j=1}^{L+1} \left| \sum_{\vec{k}} S_{\vec{k}n_j} \right|^2 . \tag{4.23}$$

From (2.30), (4.14), (4.17), and (4.19) we find that the Fano parameter is the same for all ν, i.e., $q_\nu = q$ (which is an atomiclike quantity) where

$$q = \frac{\langle d|T|p\rangle + \sum_l \mathrm{P} \int \frac{d\epsilon'}{\epsilon - \epsilon'} \left\langle p\epsilon' l \left| \frac{e^2}{r} \right| dd \right\rangle \langle \epsilon' l | T | d \rangle}{\pi \sum_l \left\langle p\epsilon l \left| \frac{e^2}{r} \right| dd \right\rangle \langle \epsilon l | T | d \rangle} . \tag{4.24}$$

We neglect the slow variation of q with ϵ.

We shall regard V as large enough that $n_{i=0\downarrow} \simeq c_1^\dagger c_1$, so that $\langle \Phi_{\alpha'} | n_{i=0\downarrow} | \Phi_\alpha \rangle \simeq 0$, $\alpha' \neq \alpha$. (We consider only those states α for which $n=1$ is occupied, since the rest have negligible absorption.) Hence we can neglect the off-diagonal elements of Γ. In this case $A_\alpha^{(\nu)} = \delta_{\alpha\nu}$ and ($\Gamma_\alpha = \Gamma_{\alpha\alpha}$)

$$z_\alpha(E) = \frac{\pi}{\Gamma_\alpha}(E - E_\alpha) . \tag{4.25}$$

The resonance shift $F_{\alpha\alpha}$ is neglected since it is insignificant in the present context.

From (2.23), (2.31), (4.14), (4.17), and (4.24), we can show that the photoemission intensity of the βth final state is for N_0 sites ($E = h\nu + E_g$; note that in this section $E_g \neq 0$)

$$N_\beta(E) = \frac{2\pi}{\hbar} N_0 t_d^2 \left[|\langle \Phi_\beta' | \Phi_g \rangle|^2 + \tau \left(\frac{\Gamma_0}{\pi} \right) |X_\beta|^2 + \frac{\tau\Gamma_0}{\pi} 2\,\mathrm{Re}(\langle \Phi_g | \Phi_\beta' \rangle X_\beta) \right] , \tag{4.26}$$

where

$$t_d^2 = \sum_l |\langle \epsilon l | T | d \rangle|^2 , \tag{4.27}$$

$$\tau = \pi \left| \sum_l \langle p\epsilon l | e^2/r | dd \rangle \langle \epsilon l | T | d \rangle \right|^2 \Big/ \Gamma_0 t_d^2 , \tag{4.28}$$

and

$$X_\beta = (q - i) \sum_\alpha \frac{\pi}{\Gamma_\alpha} \frac{\pi}{z_\alpha(E) + i\pi} \langle \Phi_\beta' | d_{i=0\downarrow} | \Phi_\alpha \rangle \langle \Phi_\alpha | d_{i=0\downarrow}^\dagger | \Phi_g \rangle . \tag{4.29}$$

The binding energy of the βth final state is [from (4.5) and (4.12)]

$$E_\beta^B = E_\beta' - E_g \tag{4.30a}$$

$$= \sum_{j=1}^{L} (\omega_{m_j} - \epsilon_{k_j\downarrow}) - \epsilon_\uparrow . \tag{4.30b}$$

The photoemission intensity as a function of binding energy $E^B = h\nu - \epsilon$ is $\sum_\beta N_\beta(E)\,\delta(E^B - E_\beta^B)$.

Likewise, the absorption is [from (2.32)]

$$W(E) = \frac{2\pi}{\hbar} N_0 t_d^2 \left(1 - \frac{\tau\Gamma_0}{\pi} \sum_\alpha \frac{\pi}{\Gamma_\alpha} |\langle \Phi_\alpha | d_{i=0\downarrow}^\dagger | \Phi_g \rangle|^2 + \frac{\tau\Gamma_0}{\pi} \sum_\alpha \frac{\pi}{\Gamma_\alpha} |\langle \Phi_\alpha | d_{i=0\downarrow}^\dagger | \Phi_g \rangle|^2 \times \frac{[q + z_\alpha(E)/\pi]^2}{[z_\alpha(E)/\pi]^2 + 1} \right) . \tag{4.31}$$

The exact sum rule (2.25) requires

$$\sum_\beta N_\beta(E) = W(E) . \tag{4.32}$$

The extent to which (4.32) actually holds for our approximation is an indication of the validity of our neglect of the off-diagonal elements of Γ.

B. Numerical results

Typical photoemission plots (in histogram form) are displayed in Fig. 2 for various photon energies. Each curve consists of a main line and a

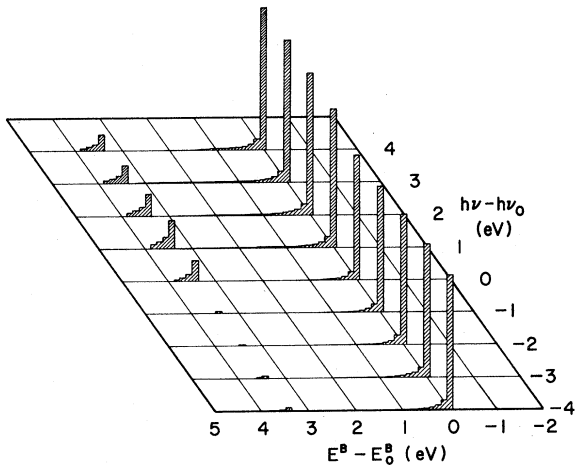

FIG. 2. Photoemission intensity vs binding energy E^B at various photon energies near resonance for the Ni model: $N_0 = 20$, $L = 16$, $V = 2.5$ eV, $U = 2.5$ eV, bandwidth = 2.5 eV, $\tau = 1$, $q = 1$, and $\Gamma_0 = 1$ eV. $h\nu_0 = E_{\alpha,\min} - E_g$. Only the $\uparrow$ emission is shown. If the $\uparrow$ bandwidth were included in the calculation, the main line, which corresponds to valence-band emission, would be broadened, but the satellite would remain nearly the same. The $\downarrow$ emission is constant as a function of $h\nu$ and is distributed in E^B according to the occupied $\downarrow$ valence-band density of states.

satellite, the latter being due to two bound holes at the origin in the final state. The excited state obtained upon absorption of a photon decays preferentially into the two-hole bound state because the Auger (SCK) matrix element has been taken to be strictly intra-atomic. Multiplet structure and the finite lifetime of the two-hole bound state, effects omitted in this model, broaden the satellite observed in Ni metal.

The absorption $W(E)$, shown in Fig. 3, has the characteristic Fano line shape. Also shown in Fig. 3 are the integrated intensities of the main line and satellite as a function of photon energy. For the model presented in this section, it is not possible to separate the photoemission into interference ($N^{(I)}$) and Auger ($N^{(A)}$) terms as in Sec. III. The integrated $\downarrow$ band emission, which is equal to $(2\pi/\hbar)Lt_d^2$, has been added to the main line (and to the absorption), since there is no $\downarrow$ satellite in this model. The different asymmetries (different effective q values) are evident. The qualitative features of these results agree with the experiment shown in Fig. 2 of Ref. 2. Interference, similar to the dip in the main line of our Fig. 3, is clearly evident in the valence-band emission of Ni. Likewise, the resonant enhancement of the satellite is observed. There is a question, however, as to the amount of asymmetry in the satellite intensity because of the overlapping $M_{2,3}VV$ Auger signal (core electron absorbed into $4s$-$4p$ conduction band). Iwan *et al.*[22] attempted a decomposition of the spectra into a satellite and an Auger term. The intensity of the satellite as a function of photon energy was found to be resonant but did not display $q>0$ asymmetry. On the other hand, the satellite intensity obtained by Guillot *et al.*[1] and by Barth *et al.*[2] (curve c, Fig. 2 of Ref. 2) is similar to our calculated satellite curve.

It is interesting to compare the results of this model with those of the band model (Sec. III) which neglects hole-hole interactions. In Fig. 4, we show the results for $N_V=1.3$, $N_B=0.2$, $N_C=2$, $W_B=0.2$ eV, $\Gamma_0=1$ eV, $q=1$, $\tau=1$, and $F_I=0$. [Note that although N_V, N_B, and N_C are smaller than realistic (for Ni $N_V\simeq 9$, $N_B\simeq 1$, $N_C=6$) this is compensated by letting Γ_0 be large (realistically $\Gamma_0\simeq 0.04$ eV).] For comparison of intensities, we note that $\sum_l t_l^2=\frac{1}{2}N_V t_d^2$ in this case. Since W_B is small, the results are nearly the same as the simplest Fano theory in which the absorption goes as $A+B(q+\mathcal{E})^2/(\mathcal{E}^2+1)$, where $\mathcal{E}=(E-E_{th})/\Gamma$. The curve for $N^{(I)}(E)$ is of the same form, except that q is smaller, a result found by Yafet.[21] The Auger curve is nearly Lorentzian and the Auger electron appears at approximately "fixed" binding energy.

The absorption curves in Figs. 3 and 4 are al-

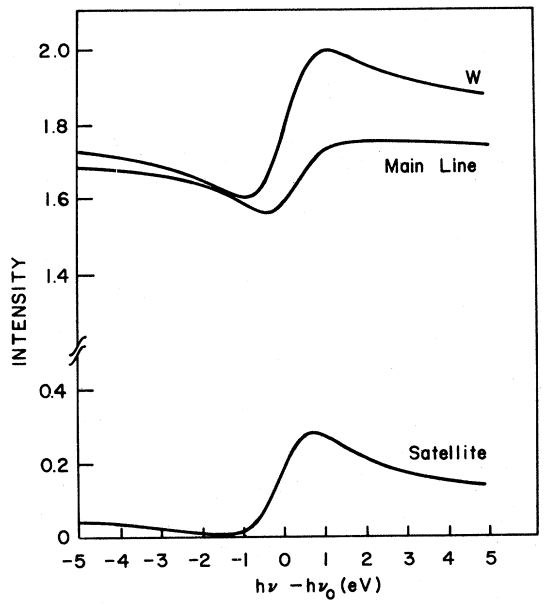

FIG. 3. Photoemission intensity (yield) and absorption in units of $(2\pi/\hbar)N_0t_d^2$ vs photon energy for the Ni model. Main line refers to the integrated intensity of the large peak in Fig. 2 plus the $\downarrow$ emission (L/N_0 in these units) not shown, whereas satellite refers to the smaller peak. The absorption W is the sum of the main line and satellite photoemission.

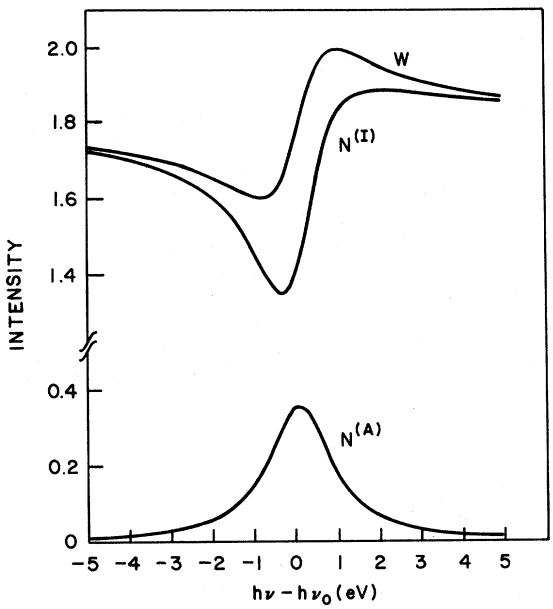

FIG. 4. Photoemission intensity (yield) and absorption in units of $(2\pi/\hbar)M_0t_d^2$ vs photon energy for band model of Ni: $N_V=1.8$, $N_B=0.2$, $N_C=2$, $W_B=0.2$ eV, $\Gamma_0=1$ eV, $q=1$, $\tau=1$, $F_I=0$, $h\nu_0=E_{th}$, and $W=N^{(I)}+N^{(A)}$.

most identical, indicating that absorption is not sensitive to hole-hole interactions in nearly filled bands. The Auger emission in Fig. 4 is similar to the satellite emission of Fig. 3, although the latter contains some asymmetry and is smaller. Also observed experimentally but not included in our model is Auger emission which occurs at fixed kinetic energy, not fixed binding energy as in the present case, arising from final states where the electron goes into the $4s$-$4p$ band.[35] The dip in the main line at resonance (Fig. 3) is similar to but weaker than in the interference term (Fig. 4).

The physical picture is now fairly well established. Near resonance, a $3p$ core electron is absorbed into the $3d$ band. Owing to the core hole potential, the charge density is approximately $3p^5 3d^{10}$. Super-Coster-Kronig decay results in two $3d$ holes which may be localized (bound) on the same site, giving rise to satellite emission and the $3p^6 3d^8$ configuration, or may be free and extended throughout the crystal. The latter corresponds to the two-hole continuum in the Auger problem considered by Sawatzky[20] and Cini.[36] This emission occurs at lower binding energy than the satellite and interferes with the main line (valence band) emission. The stronger the hole-hole interaction, however, the more the interference would occur in the satellite because of the preferential decay into the two-bound-hole final state.

V. APPLICATION TO Cu, Zn, ETC.

A. Description of model

The model presented in this section has been described previously.[24] The notation differs slightly to be consistent with previous sections and an error in Eq. (11) of Ref. 24 is corrected. The purpose is to show that resonant photoemission can occur even though the $3d$ bands are full. Zn is a good example of a real metal to which our model applies, since the $3d$ bands are well below the Fermi level. Cu is another example, although hybridization causes some $3d$ character above the Fermi level. This may make Cu somewhat like Ni. Dietz *et al.*[15] have shown that interference effects occur at the $3p$ absorption threshold, which suggests the importance of the $3d$ component of the empty states above the Fermi level. However, away from resonance, the excitation of the two-hole satellite is weak, in contrast to Ni.

We consider only a single conduction band (analogous to the $4s$-$4p$ bands) into which the $3p$ core electron is excited when a photon is absorbed. In the ground state, the Hamiltonian for the $4s$-$4p$ electrons is $H_0 = \sum_{\vec{k}} \epsilon_{\vec{k}} c_{\vec{k}}^\dagger c_{\vec{k}}$. For simplicity, we neglect spin. The ground state is $b^\dagger|\Phi_g\rangle$, where now $|\Phi_g\rangle = \prod_{j=1}^{L} c_{\vec{k}_j}^\dagger |0\rangle$. The ground state energy is $E_g = \sum_{j=1}^{L} \epsilon_{\vec{k}_j} + \epsilon_c$. Following absorption, the Hamiltonian consists of H_0 plus an interaction term due to the hole in the core level:

$$H = \sum_{\vec{k}} \epsilon_{\vec{k}} c_{\vec{k}}^\dagger c_{\vec{k}} - \frac{U_S}{N_0} \sum_{\vec{k}} c_{\vec{k}}^\dagger \sum_{\vec{k}'} c_{\vec{k}'}\,, \tag{5.1}$$

where U_S is a parameter describing the strength of the interaction. H can easily be diagonalized using (4.9) with V replaced by U_S:

$$H = \sum_n \omega_n c_n^\dagger c_n\,, \tag{5.2}$$

where now $c_{\vec{k}} = \sum_n S_{\vec{k}n} c_n$. The discrete states ($\phi_n$ of Sec. II) of the system are

$$|\phi_\alpha\rangle = \prod_{i=1}^{L+1} c_{n_i}^\dagger |0\rangle\,, \tag{5.3}$$

where α stands for $\{n_1, n_2, \ldots, n_{L+1}\}$. The energy is

$$E_\alpha = \sum_{i=1}^{L+1} \omega_{n_i}\,. \tag{5.4}$$

These states decay by super-Coster-Kronig transitions into continuum states with the core level filled but with two $3d$ holes bound at the origin (the $3d^8$ configuration).[37] Here we neglect dispersion of the two-hole state as well as its multiplet structure. The Hamiltonian for the conduction-band electrons in the presence of the two holes is the same form as (5.1), but with U_S replaced by U_S' which we expect to be much larger (U_S corresponds to $Z=1$ and U_S' to $Z=2$). Let us denote the eigenvalues and eigenvectors by ω_n' and $S_{\vec{k}n}'$, etc. The continuum states (ψ_{kE} of Sec. II) are denoted by $|\psi_{\beta E}\rangle$ where

$$|\psi_{\beta E}\rangle = b^\dagger |\epsilon\, d^8 \phi_\beta'\rangle\,, \tag{5.5}$$

ϵ stands for the photoemitted electron (for simplicity we do not consider its orbital symmetry), d^8 signifies the two-hole state, and

$$|\phi_\beta'\rangle = \prod_{i=1}^{L+1} c_{m_i}'^\dagger |0\rangle\,. \tag{5.6}$$

Here β stands for $\{m_1, m_2, \ldots, m_{L+1}\}$ and the energy of $|\psi_{\beta E}\rangle$ is

$$E = \epsilon + \epsilon_c + E(d^8) + E_\beta'\,, \tag{5.7}$$

with

$$E_\beta' = \sum_{i=1}^{L+1} \omega_{m_i}'\,. \tag{5.8}$$

The energy for the creation of two bound holes is $E(d^8)$.

The matrix element (V_{kn} of Sec. II) for the decay of the discrete state $|\phi_\alpha\rangle$ into the continuum state $|\psi_{\beta E}\rangle$ is

$$V_{\beta\alpha}(E) = V_0 \langle \phi'_\beta | \phi_\alpha \rangle . \tag{5.9}$$

Here $V_0 \sim \langle 3p\epsilon l | e^2/r | 3d3d \rangle$, the super-Coster-Kronig matrix element. (We neglect its dependence on ϵ.) The total decay rate of ϕ_α into all continuua is $\Gamma_0 = \pi |V_0|^2$.

The photoemission intensity $N(h\nu, \epsilon)$ can be calculated from (2.23) and (2.27). In this case, $\langle \psi_{kE} | T | \Phi_g \rangle = 0$ for all continua, since there is no direct excitation of the d^8 final states. The result is (multiply by N_0 for all sites)

$$N(h\nu, \epsilon) = \frac{2\pi}{\hbar} \left| \sum_\alpha \frac{\pi}{\Gamma_0} \frac{1}{z_\alpha + i\pi} \langle \phi_\alpha | T | \Phi_g \rangle V_{\beta\alpha} \right|^2 \times \delta(h\nu + E_g - \epsilon - \epsilon_c - E(d^8) - E'_\beta), \tag{5.10}$$

where

$$z_\alpha = \pi (h\nu + E_g - E_\alpha)/\Gamma_0 \tag{5.11}$$

and $\langle \phi_\alpha | T | \Phi_g \rangle$ has the same form as (4.19) and (4.20) with $\langle d | T | p \rangle$ replaced by $\langle s | T | p \rangle$. The essential feature of (5.10) is the adding of amplitudes for the excitation of the βth final state before squaring. The rate of absorption is [using (5.9) and (5.10)]

$$W(h\nu) = \int d\epsilon N(h\nu, \epsilon) = \frac{2\pi}{\hbar} \frac{\pi}{\Gamma_0} \sum_\alpha \frac{1}{z_\alpha^2 + \pi^2} |\langle \phi_\alpha | T | \Phi_g \rangle|^2 . \tag{5.12}$$

Threshold is at $h\nu_0 = E_{\alpha,\min} - E_g = -\epsilon_c + \sum_{n=1}^{L+1} \omega_n - \sum_{j=1}^{L} \epsilon_{\tilde{k}_j}$, where $E_{\alpha,\min}$ is the lowest E_α. From (5.10), we see that the possible values of binding energy are

$$E^B_\beta = E(d^8) + E'_\beta - \sum_{j=1}^{L} \epsilon_{\tilde{k}_j} . \tag{5.13}$$

The lowest binding energy is $E^B_0 = E(d^8) + \sum_{m=1}^{L+1} \omega'_m - \sum_{j=1}^{L} \epsilon_{\tilde{k}_j}$, which corresponds to the d^8 satellite (the last two terms represent the relaxation of the conduction electrons around the two bound holes). We can rewrite (5.10) as

$$N(h\nu, \epsilon) = \frac{2\pi}{\hbar} \sum_\beta \left| \sum_\alpha \frac{\pi}{\Gamma_0} \frac{1}{z_\alpha + i\pi} \langle \phi_\alpha | T | \Phi_g \rangle V_{\beta\alpha} \right|^2 \times \delta(E^B - E^B_\beta) . \tag{5.14}$$

In Ref. 24, we remarked that $N(h\nu, \epsilon) \sim 1/(E^B - E^B_0)^\lambda$ as $E^B \to E^B_0$. We can derive the limiting form of (5.14) for $|h\nu - h\nu_0| \gg \Gamma_0$ by replacing z_α by

$$\bar{z} = \sum_\alpha |\langle \phi_\alpha | T | \Phi_g \rangle|^2 z_\alpha \Big/ \sum_\alpha |\langle \phi_\alpha | T | \Phi_g \rangle|^2 .$$

Using (5.9) and the completeness of $|\phi_\alpha\rangle$, we find

$$N(h\nu, \epsilon) \simeq \frac{2\pi}{\hbar} \frac{\pi}{\Gamma_0} \frac{1}{\bar{z}^2 + \pi^2} \sum_\beta |\langle \phi'_\beta | T | \Phi_g \rangle|^2 \delta(E^B - E^B_\beta) . \tag{5.15}$$

Now

$$\bar{W}(E) \equiv \frac{2\pi}{\hbar} \sum_\beta |\langle \phi'_\beta | T | \Phi_g \rangle|^2 \delta(E - E^B_\beta) \tag{5.16}$$

is the absorption of the core level into the $4s$-$4p$ band if the core hole has a potential U'_S instead of U_S. The singular behavior of $W(E)$ is $(E - E^B_0)^{-\lambda}$, where[38] (for a single spinless band)

$$\lambda = 2\delta'/\pi - (\delta'/\pi)^2 . \tag{5.17}$$

The phase δ' is determined by U'_S.

B. Numerical results

Calculations for the model presented in this section are displayed in Figs. 5 and 6 for a constant density of states with the band half filled. In Fig. 5, we plot $N(h\nu, E^B)$ vs E^B for various $h\nu$ near threshold, $h\nu_0$. (This is a corrected version of Fig. 1 in Ref. 24.) The valence-band emission is not shown, only the satellite and Auger peaks. The latter moves to larger binding energy as $h\nu$ is increased, since the kinetic energy ϵ_A of the Auger electron is fixed (recall $E^B_A = h\nu - \epsilon_A$). The satellite persists well above resonance because of the singular behavior of $N(h\nu, E^B)$. The integrated intensities of the Auger peak and the satellite are shown in Fig. 6; the absorption is also shown. These results are in qualitative agreement with the results of Iwan, Himpsel, and Eastman.[22]

The mechanism has features which may possibly be tested experimentally. The width of the satel-

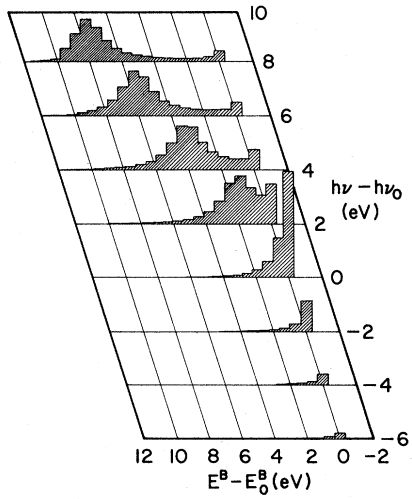

FIG. 5. Photoemission intensity vs binding energy at various photon energies near resonance for Cu model. Calculation for half-filled uniform band, $\epsilon_F = 10$ eV, $U_S = 0$, $U'_S = 10$ eV, $\Gamma_0 = 1$ eV, and $N_0 = 32$. Only the satellite (lowest-binding-energy peak) and the Auger emission (peak which moves to larger E^B with increasing $h\nu$) are shown.

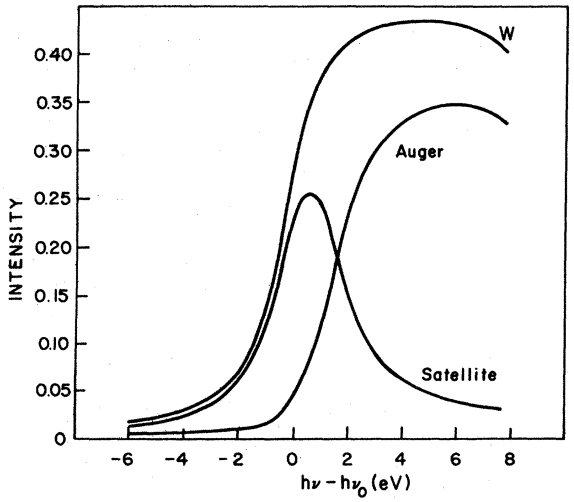

FIG. 6. Photoemission intensity (yield) and absorption in units of $(2\pi/\hbar)N_0\langle s|T|p\rangle^2/\epsilon_F$ vs photon energy for Cu model. Satellite refers to the total intensity of the first three channels (lowest E_B) in Fig. 5. W represents the $3p \rightarrow 4s$-$4p$ band absorption. The absorption W exceeds the sum of the Auger and satellite photoemission slightly, due to final states (mostly at high energy) which have been omitted in the photoemission calculation. The decrease in W and the Auger intensity near 8 eV results from the finite width of the band. Absorption and photoemission due to the filled $3d$ bands and occupied $4s$-$4p$ bands are omitted.

lite peak (actually two peaks due to multiplet splitting) is governed by the lifetime of the $3d^8$ configuration, but does not contain the $3p$ hole lifetime broadening or the $3p$ spin-orbit splitting. Also, there is some asymmetry in the satellite (tailing to higher binding energy) according to our model.

VI. CONCLUSIONS

We have presented three model calculations which illustrate the essential features of resonant photoemission involving super-Coster-Kronig transitions in the $3d$ metals. For metals in which the $3d$ bands are not completely filled, absorption into the d bands followed by the decay of the $3p$ core hole can interfere with the direct excitation of the valence band. If a single-particle (band) picture is valid, as it may be for certain aspects of Cr, then the decay can be separated into two parts: (i) a coherent term (which results from the direct recombination of the electron absorbed from the $3p$ core level into the $3d$ band) that causes interference mostly of the form of a dip (i.e., small-q Fano resonance); and (ii) an incoherent term due to Auger processes. When electron-electron interactions become important, the Auger intensity occurs at higher binding energy because of the $3d$ hole-hole repulsion. In Ni it occurs mostly in the satellite region. Asymmetry of the satellite peak is due to interference between direct satellite excitation and decay of the $3p$ hole. The strong Auger component, however, causes the q of the peak to be large.

In metals with filled $3d$ bands, a new mechanism, which involves the singular response of the $4s$-$4p$ bands to the d^8 configuration in the final state, becomes important. In Cu, the presence of hybridized $3d$ states above ϵ_F may also be important because of the enhanced oscillator strength associated with transitions of $3p$ to states near ϵ_F. The semiconductor GaP is interesting because the satellite final state corresponds to an exciton consisting of $3d^8$ plus a screening (bound) electron below the Γ_1 or L_1 conduction-band minima.[28] By introducing a gap in the density of states at the Fermi level, the model presented in Sec. V can also describe the semiconductor case.

In Ni-phthalocyanine[30] and NiO,[29] the resonance can be analyzed in terms of the Ni^{2+} ion, where $3p^63d^8 + h\nu \rightarrow 3p^63d^9 \rightarrow 3p^63d^7\epsilon l$ interfering with $3p^63d^8 + h\nu \rightarrow 3p^63d^7\epsilon l$. Here we would expect the resonance to be associated with final states of the $3d^7$ configuration (the main line). Apparently the multielectron satellite shows a strong enhancement. It is possible that the O^{2-} $2p$ bands in NiO play a role.

ACKNOWLEDGMENTS

We wish to thank Dr. R. E. Dietz and Dr. D. R. Penn for helpful conversations and comments and Dr. Y. Yafet for communicating his results prior to publication.

[1] C. Guillot, Y. Ballu, J. Paigné, J. Lecante, K. P. Jain, P. Thiry, R. Pinchaux, Y. Pétroff, and L. M. Falicov, Phys. Rev. Lett. 39, 1632 (1977).
[2] J. Barth, G. Kalkoffen, and C. Kunz, Phys. Lett. 74A, 360 (1979).
[3] R. E. Dietz, E. G. McRae, Y. Yafet, and C. W. Caldwell, Phys. Rev. Lett. 33, 1372 (1974).
[4] U. Fano, Phys. Rev. 124, 1866 (1961).
[5] B. Sonntag, R. Haensel, and C. Kunz, Solid State Commun. 7, 597 (1969).
[6] F. C. Brown, C. Gähwiller, and A. B. Kunz, Solid State Commun. 9, 487 (1971).
[7] M. B. Stearns and L. A. Feldkamp, in *Magnetism and Magnetic Materials—1975 (Philadelphia)*, Proceedings

of the 21st Annual Conference on Magnetism and Magnetic Materials, edited by J. J. Becker, G. H. Lander, and J. J. Rhyne (AIP, New York, 1976), p. 286.
[8]L. C. Davis and L. A. Feldkamp, Solid State Commun. 19, 413 (1976).
[9]C. Wehenkel and B. Gauthé, Phys. Lett. 47A, 253 (1974); Phys. Status Solidi B 64, 515 (1974).
[10]E. J. McGuire, Phys. Rev. A 5, 1052 (1972); Sandia Laboratories Report No. SC-RR-71 0835 (unpublished); J. Phys. Chem. Solids 33, 577 (1972).
[11]J. P. Connerade, M. W. D. Mansfield, and M. A. P. Martin, Proc. A. Soc. London Ser. A 350, 405 (1976).
[12]L. C. Davis and L. A. Feldkamp, Phys. Rev. A 17, 2012 (1978).
[13]R. Bruhn, B. Sonntag, and H. W. Wolff, Phys. Lett. 69A, 9 (1978); J. Phys. B 12, 203 (1979).
[14]F. Combet Farnoux and M. Ben Amar, Phys. Rev. A 21, 1975 (1980).
[15]R. E. Dietz, E. G. McRae, and J. H. Weaver, Phys. Rev. B 21, 2229 (1980).
[16]D. R. Penn, Phys. Rev. Lett. 42, 921 (1979).
[17]A. Liebsch, Phys. Rev. Lett. 43, 1431 (1979); Phys. Rev. B (in press).
[18]L. C. Davis and L. A. Feldkamp, J. Appl. Phys. 50, Pt. 2, 1944 (1979).
[19]L. C. Davis and L. A. Feldkamp, Solid State Commun. 34, 141 (1980).
[20]G. A. Sawatzky, Phys. Rev. Lett. 39, 504 (1977). Also see G. A. Sawatzky and A. Lenselink, Phys. Rev. B 21, 1790 (1980).
[21]Y. Yafet, Phys. Rev. B 21, 5023 (1980).
[22]M. Iwan, F. J. Himpsel, and D. E. Eastman, Phys. Rev. Lett. 43, 1829 (1979).
[23]D. E. Eastman, J. F. Janak, A. R. Williams, R. V. Coleman and G. Wendin, J. Appl. Phys. 50, Pt. 2, 7423 (1979).
[24]L. C. Davis and L. A. Feldkamp, Phys. Rev. Lett. 44, 673 (1980).
[25]S. M. Girvin and D. R. Penn, Phys. Rev. B 22, 4081 (1980).
[26]J. Barth, F. Gerken, K. L. I. Kobayshi, J. H. Weaver and B. Sonntag, J. Phys. C 13, 1369 (1980).
[27]F. J. Himpsel, D. E. Eastman, and E. E. Koch, Phys. Rev. Lett. 44, 214 (1980) and private communication.
[28]T.-C. Chiang and D. E. Eastman, Phys. Rev. B 21, 5749 (1980).
[29]I. Lindau, Bull. Am. Phys. Soc. 25, 358 (1980) and private communication; Se-Jung Oh, I. Lindau, and J. C. Mikkelsen, Bull. Am. Phys. Soc. 26, 461 (1981).
[30]M. Iwan and E. E. Koch, Solid State Commun. 31, 261 (1979).
[31]M. Iwan, E. E. Koch, T.-C. Chiang, D. E. Eastman, and F. J. Himpsel, Solid State Commun. 34, 57 (1980).
[32]L. C. Davis and L. A. Feldkamp, Phys. Rev. B 15, 2961 (1977).
[33]G. Wendin, Daresbury Nuclear Laboratory Report No. DL/SCI/R11, (unpublished); G. Wendin and K. Nuroh, Bull. Am. Phys. Soc. 24, 367 (1979) and unpublished report. Wendin and Nuroh use the term super-Coster-Kronig strictly to mean decay with electrons emitted at well-defined kinetic energies independent of photon energy. Our use of that term is based upon the matrix element involved and includes some processes that Wendin and Nuroh would call autoionization.
[34]L. I. Yin, T. Tsang, and I. Adler, Phys. Rev. B 15, 2974 (1977).
[35]M. M. Traum, N. V. Smith, H. H. Farrell, D. P. Woodruff, and D. Norman [Phys. Rev. B 20, 4008 (1979)] measured the angle dependence of the emission from the 6-eV satellite on Ni(100) near resonance. They noted the similarity of their data to electron-stimulated *MVV* Auger data [S. P. Weeks and A. Liebsch, Surf. Sci. 62, 197 (1977)] and concluded that most of the enhancement of the satellite at resonance is due to Auger emission. At resonance, the core electron is excited to the $3d$ band, whereas in the electron-stimulated *MVV* Auger experiment the core electron is excited well above the $3d$ band. In both cases, however, the local electronic configuration is approximately $3p^5 3d^{10}$ [see L. A. Feldkamp and L. C. Davis, Phys. Rev. B 22, 3644 (1980) and Phys. Rev. Lett. 43, 151 (1979)] and the resulting decay to $3p^6 3d^8 \epsilon l$ is nearly identical in the two cases. Hence it may not be so surprising that the angle dependence is similar. Well away from resonance, the angle dependence of the 6-eV satellite does not involve Auger (SCK) matrix elements and could well be different.
[36]M. Cini, Solid State Commun. 24, 681 (1977); Phys. Rev. B 17, 2788 (1978).
[37]E. Antonides, E. C. Janse, and G. A. Sawatzky, Phys. Rev. B 15, 1669 (1977).
[38]P. Nozières and C. T. de Dominicis, Phys. Rev. 178, 1097 (1969).